

Electrochemical Properties and Calcareous Deposits Formation under Cathodic Polarization on Stainless Steel in Seawater

Propriedades eletroquímicas e Formação de Depósitos Calcários sob Polarização Catódica em Aço Inoxidável na Água do Mar

F. Hedaiat

Department of Materials Science, Faculty of Engineering, Behbahan Branch, Islamic Azad University

Abstract:

The optimum corrosion prevention conditions for cathodic protection of 316 stainless steels were determined by accelerated electrochemical and immersion tests. Tests were devised to examine the influence of applied cathodic potential and biofilms on calcareous deposits formation and growth. Results showed that passivity characteristic of 316 was better than 304. Pitting and repassivation potential of 316 and 304 stainless steels were 312, -215 and 330 and -210 mV (SCE) respectively. Polarization diagrams showed, for corrosion protection need a potential more negative than -650mV (SCE). Funding showed that calcareous deposits decrease the current needs to achieve complete protection and caused an important decrease of galvanic corrosion rates for sacrificial anodes. Calcareous deposits developed rapidly on the SS cathodes and led to a significant reduction of bacterial numbers in the initial stages of biofilms formation. The deposits were composed of carbonates, oxides and hydroxides of calcium and magnesium. At potentials more negative than -700mV, the deposition of magnesium was relatively higher than calcium. Data from this work suggest that a potential of about -700 mV (SCE) should provide optimum protection of SS in natural seawater that support the precipitation of calcareous deposits. Bacterial biofilms changed the morphology of calcareous deposits.

Keywords: Stainless Steel, Cathodic Protection, Calcareous Deposits, Biofilm, Sacrificial Anodes, Seawater

Resumo:

As melhores condições de prevenção da corrosão para proteção catódica do aço inoxidável 316 foram determinadas por eletroquímica acelerada e testes de imersão. Os testes foram planejados para examinar a influência da aplicação de potencial catódico e biofilmes na formação e no crescimento de depósitos calcários. Os resultados mostraram que a característica da passividade de aço inoxidável 316 era melhor do que a do 304. Potenciais de pite e de repassivação dos aços inoxidáveis 316 e 304 foram 312, -215 e -210 e 330 mV (SCE), respectivamente. Diagramas de polarização mostraram que para proteção contra corrosão é necessário um potencial mais negativo do que -650mV (SCE). Depósitos de produtos calcários são eficazes em diminuir as necessidades para conseguir uma proteção completa e causaram uma diminuição importante da taxa de corrosão galvânica para anodos de sacrifício. Depósitos calcários se desenvolveram rapidamente nos catodos de aço inoxidável e levaram a uma redução significativa do número de bactérias nas fases iniciais da formação de biofilmes. Os depósitos eram compostos de carbonatos, óxidos e hidróxidos de cálcio e magnésio. Em potenciais mais negativos que -700mV, a deposição de magnésio foi relativamente maior do que o cálcio. Os dados deste trabalho sugerem que um potencial de cerca de -700 mV (SCE) devem proporcionar uma proteção ótima dos aços inoxidáveis na água do mar natural que suportam a precipitação de depósitos calcários. O biofilme bacteriano alterou a morfologia dos depósitos de calcário.

Palavras-chave: Aço Inoxidável, Proteção Catódica, Depósito Calcário, Biofilme, Anodos de Sacrifício, Água do Mar

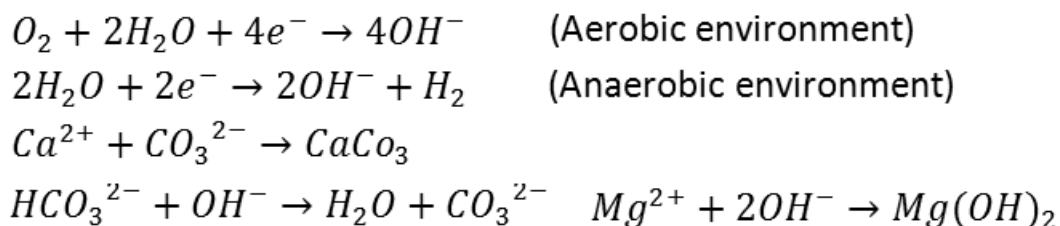
Introduction:

Cast and wrought austenitic Stainless steels are used in various applications in marine equipment [Sedriks 1996]. However, type AISI 316 considered one of the most common corrosion resistant alloys in its class, and it has a good mechanical properties, and easy fabricability, and therefore, is important material for many industrial units includes desalination plants, costal power, power plants and shipboard [Sedriks 1996; Jones 1996]. The most common failure in stainless steels is the breakdown of passivity in chloride containing environments, which leads to localize corrosion in a form of pitting, crevice and intergranular corrosion. Stress corrosion cracking (SCC) or sulphide Stress corrosion cracking (SSCC) may also occur [Johnsen 1985]. The breakdown of passivity during crevice corrosion has been attributed to reduce pH in a crevice [Little 1993], but with pitting; there is, in general, no clearly explained the cause of the initial breakdown [Habib 2000]. Normal practice is therefore, to avoid conditions where local attacks may begin, or prevent towards corrosion by e. g. cathodic protection [Jones 1996]. Cathodic protection is a widely used method in marine environments and certain soil where the medium conductivity is high enough to establish a uniform current distribution over the metal surface to be protected [Sedriks 1996; Jones 1996].

Cathodic protection of stainless steel can be obtained at far more positive potential than carbon steel. For these materials, cathodic protection can be effective even with little higher protection potentials (-700 mV SCE) or by simple coupling to low carbon steel anodes [Lee 1988; Hedaiat 2005]. Some investigators reported current density needed for protection about 80-120 $\frac{\text{mA}}{\text{m}^2}$ [Hedaiat 2005; Lee 1988; Eliassen 2004]

Others recent studies have shown that in order to prevent localized corrosion on stainless steel, it is enough to hold the potential in the lower passive region ($\pm 250\text{mV SCE}$), but for prevent corrosion of pre-existing active pit or crevice, Cathodic polarization more negative than protection potential has been needed [Hedaiat 2005, Lee 1988; Little 1993]. Fouling and calcareous deposits that can grow in marine environments have significant effects on the cathodic protection efficiency. Calcareous deposits on iron have a protective action [Lye 1988].

Cathodic protection alters the ionic concentration at the interface, increasing the hydroxyl ion concentration [Sarлак 2005; Weing 2007]. The consequent pH increase reduces the solubility of calcium, magnesium and bicarbonate ions at the interface favouring the precipitation of a calcareous scale according to the following reactions:



The ease of growing calcareous deposits on passive metals can be more difficult than has been observed carbon steel. Some authors have not viewed the growth of calcareous deposits on cathodically protected SS in seawater while other authors have [Dexter 1991; Johnsen 1985; Luo 1991; Mele 1994; Sarлак 2009; Scotto 1985].

The growth of calcareous deposits can interact in different ways with biofilms still present on the surfaces. Some bacteria can cause their dissolution. Some deposits can be disbanded from surfaces, and surface acidification can occur even under cathodic protection. Deposits lead to an increase of concentration polarization values and promote the effectiveness of cathodic protection. Porous deposits could become harmful with cathodic protection current blackout [Dexter 1989; Dickinson 1996].

It is well accepted that natural biofilms lead to an ennobling of the open-circuit potentials for stainless steel alloys by a few hundred to several hundreds of millivolts [Malik 1994; Oldfield 1987]. Biofilms increased cathodic properties and favours the initiation and propagation of crevice attack by at less corrosion resistant stainless steels [Mele 1994]. In the presence of biofilms need greater current density for cathodic protection [Dexter 1991].

In the present work, the optimum cathodic protection conditions determined by electrochemical and immersion tests and the effects of biofilms on the cathodic behaviour of type-316 SS during galvanic coupling with low carbon steel and zinc in natural seawater was examined. Laboratory experiments were carried out to determined effects of biofilms and applied cathodic potential on calcareous deposits.

Experimental Procedures:

Materials:

Types UNS 304 and UNS 316 were considered as cathode materials in this work and Low carbon steel (LS) and zinc (Zn) were used as sacrificial anodes. Sheets with 2mm thickness were cut into coupons of desired sizes, mechanically polished with different grits silicon carbide metallurgical paper (180, 220, 400, and 600), cleaned and degreased with acetone and finally rinsed with distilled water before to exposure. Table1 gives the chemical composition of alloys.

Table 1 Nominal compositions of the alloys tested in the present work.

<i>Materials</i>	<i>C</i>	<i>Mn</i>	<i>P</i>	<i>S</i>	<i>Si</i>	<i>Cr</i>	<i>Ni</i>	<i>Mo</i>
AISI 316	0.08	2	0.03	0.06	1	18	10	-
AISI 304	0.08	2	0.03	0.06	1	19	12	2.3
AISI 1010	0.11	0.05	0.04	0.05	-	-	-	-
St37	0.22	0.06	0.03	0.04	-	-	-	-
<i>Materials</i>	<i>Fe</i>	<i>Si</i>	<i>Pb</i>	<i>Cu</i>	<i>Al</i>	<i>Zn</i>	<i>Hg</i>	<i>Cd</i>
Zinc	0.005	-	0.006	0.005	0.2	Balance	-	-

Galvanic corrosion set up:

All studies reported in this article were performed in the laboratory under low light conditions. Two series of tests were conducted with a constant cathode-to-anode area ratio of 10:1 and identical experimental conditions, including flow rate. In the first series of tests, Galvanic corrosion tests for low carbon steel (LS) and zinc (Zn) coupled to 304 and 316 SS were performed in separate series of tanks and rates of corrosion determined by weight loss. The SS cathodes had exposed areas of 10 cm *10 cm. The distance between the cathodes to the anode was 8 cm and connected to each other's by copper lead junctions coated with marine epoxy to avoid galvanic action from moisture. An effect of biofilms on galvanic corrosion was assessed in a manner similar to that employed by Dexter and LaFontaine and Ruppel et al. (2001). One set of galvanic couples remained connected throughout the exposure allowing biofilm development. In the other, cathodes were changed every 24 h.

Another set of SS samples was exposed, which remained uncoupled throughout the immersion period. The potentials of the uncoupled SS samples together with the mixed potentials of the different couples were measured daily using a high impedance voltmeter (Tektronix, Model DMM155) with an SCE. Zero impedance ammeter used for current measurements. After immersion in the seawater flow system for 64 days, the couples were disconnected. The anodes were removed, cleaned in respective solutions and reweigh for estimating weight loss.

In the second series of tests, smaller samples were used wherein the cathodes and anodes had immersed areas of 25 mm * 100 mm and 12.5 mm * 25 mm, respectively. The portions of coupons above the waterline (25 mm * 25 mm and 12.5 mm * 12.5 mm flags, respectively) provided room for copper electrical leads with alligator clips. Couples of SS with Mg, LS and Zn were immersed in separate sets of the seawater flow tanks as previously described. Here, the couples remained connected throughout the exposure. Uncoupled SS samples, in addition, were also exposed to the flow system as added controls. The uncoupled SS samples as well as the cathodes were used for bacterial counting and characterization and potentiodynamic polarization studies after exposure to the flow system for 65 days.

Biofilms:

Samples were washed in sterile artificial seawater and biofilms removed by scraping with a sterile nylon brush and transferred to a tube with 10 ml of autoclaved sterile seawater. Enumeration of cells was carried out by the dilution to extinction method (King, 1995).

Potentiostatic test:

SS samples were cathodically polarized from -650 mV to about -1350 mV. The electrochemical measurements were performed with a potentiostat (PARC EG&G model 273) with platinum as counter electrode and SCE as reference. The electrochemical cell had a volume of 1 litre and freshly collected seawater was used as the electrolyte after 0.26 mm Millipore filtration.

Anodic polarization experiments were carried out at room temperature using an electrochemical apparatus consisting of a Pt coil as the counter-electrode and an SCE reference. A scan rate of 2 mV/s was executed from an open circuit potential (OCP) to a voltage 3.0 V. Cathodic polarization experiments were performed from an OCP to -2.0 V. Tafel analysis was performed under both anodic and cathodic conditions from an OCP to ± 0.25 V under aerated conditions. The corrosion potential and corrosion current density was compared with Tafel analytical results obtained from various reference specimens. Potentiostatic experiments at an applied potential of 0.4 V were also performed and the resulting surface morphologies were examined and compared.

Cyclic polarization was carried out at a scan rate 1mV/S from -100 to 1200 mV with respect to corrosion potential for measuring pitting potential and repassivation potential.

Results and discussion:

Figure 1 presents the open-circuit potential (OCP) trends for the control SS samples together with the mixed potentials for the various couples. Uncoupled control SS samples exhibited typical ennobling of OCP, reaching steady values between +277 and +288 mV (SCE) after immersion for 1 week all the way through the entire experimental period of 64 days. The couples' potentials did not show important variation in corrosion potential trends depending on whether or not the cathode member accrued natural marine biofilms.

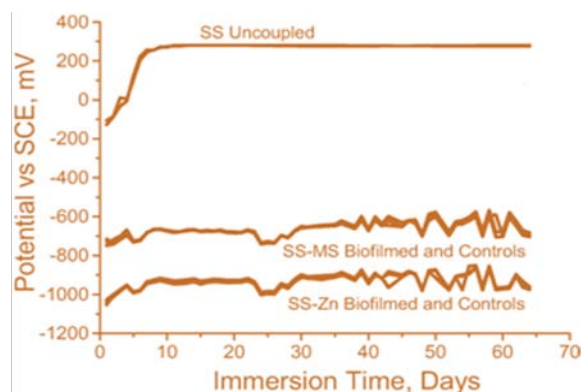


Fig.1. Potentials of various stainless steels in seawater

The results of the Tafel analysis are listed in Table 3. Anodic corrosion protection is performed at a potential lower than the pitting potential, while cathodic corrosion protection is performed at a potential higher than the hydrogen gas generation potential. The current density in the protection potential range for cathodic protection is greater than that for anodic protection, which implies that anodic protection is more useful than cathodic protection from an economic point of view. Recommended protection potential for natural seawater obtained from this analysis is about -700 mV (SCE). Figure 2 shows potentiodynamic polarization curve for stainless steels in seawater at different conditions.

Table 2 Results obtained from Tafel analysis of STS 304 and 316 stainless steels in seawater

Materials	Corrosion potential (mV)	Corrosion current Density ($A \cdot cm^{-2}$)	Repassivation potential (mV)	Pitting potential (mV)
304	-165	1.77×10^{-7}	-210	330
316	-130	3.74×10^{-8}	-215	312

The condition of the test samples was carefully observed by visual inspection throughout the exposure tests. The rates of corrosion of the anode members in the couples with and without biofilm development on the cathode surfaces showed that low steel anodes suffered higher corrosion rates without biofilms. There was no significant variation in the corrosion rate of Zn anodes between the controls and the biofilmed. Calcareous deposits developed rapidly in the couples with LS and Zn. Figure 3 showed the rate of corrosion for sacrificial anodes in the couples with and without biofilm development on the cathode surface.

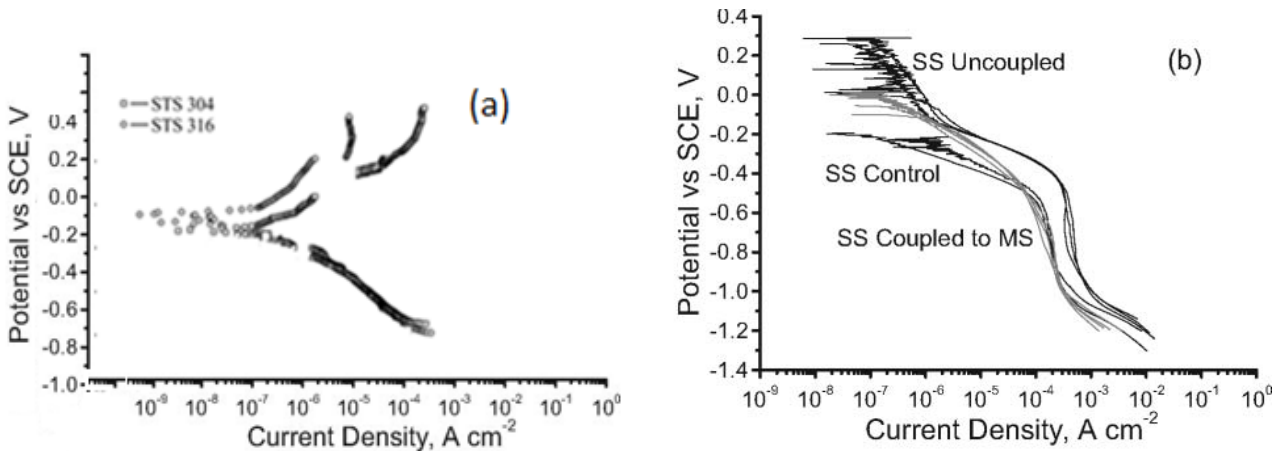


Fig.2. (a) Potentiodynamic polarization for stainless steels in artificial seawater (b) Potentiodynamic cathodic polarization curves for 316 SS exposed to seawater under various conditions and anodic polarization curves for LS.

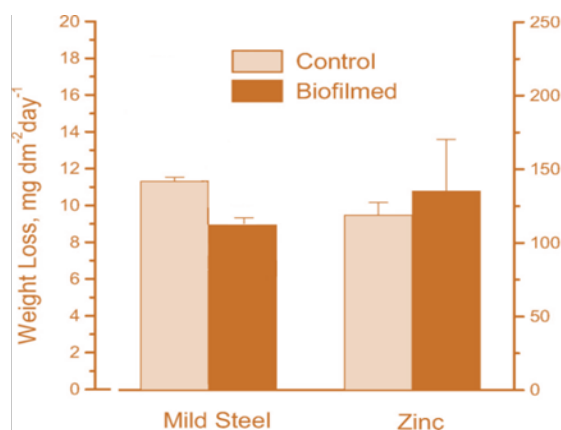


Fig.3. Corrosion rate of anode members coupled to SS with or without biofilm development obtained from weight loss measurements.

The character of the calcareous deposits as analysed by XRD is given in Figure 4. The compounds were identified as CaCO₃ (calcite, aragonite and vaterite), MgCO₃ (magnesite), Mg(OH)₂ (brucite) and MgO (brucite). With particular reference to CaCO₃, more aragonite phases were recorded than calcite or vaterite.

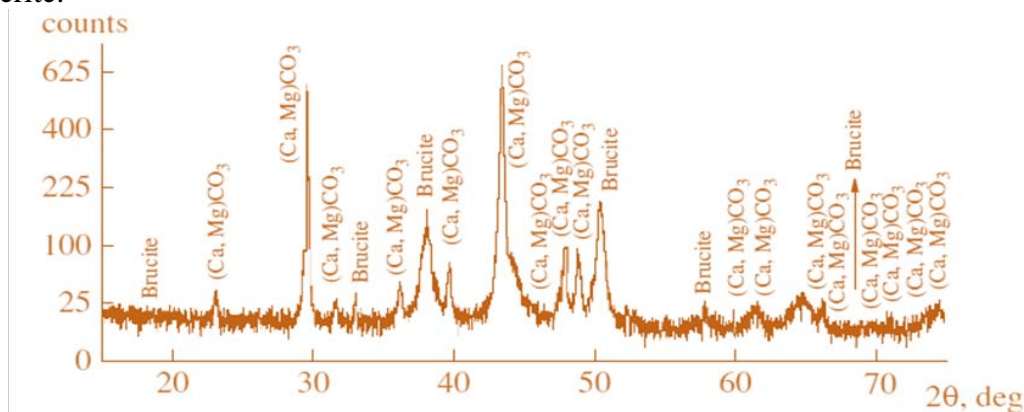


Fig.4. XRD results for small SS sample polarized to -700 V (SCE) for 100 h in natural seawater revealing the forms of calcium and magnesium compounds in the calcareous deposit.

SEM images of biofilms and calcareous deposits on the control and cathode SS samples after 100 h immersion in seawater is shown in Figure 5 a, b, respectively. The control SS sample (Figure 5a) showed aggregates of bacteria and isolated diatom cells, despite the lowlight conditions in the experimental setup.

Figure 6 shows the X-ray diffraction patterns of the deposits obtained at potentials of -1100 and -1250 mV (SCE) on stainless steel. Clearly, that the amount of brucite increases by shifting the potential toward the more cathodic potentials (-1250mV/SCE) and the Ca rich phases (aragonite and calcite) are being eliminated. Applied potential, biofilms, current density, and pH have all been demonstrated to influence the kinetics of deposit formation and thus their properties and morphologies.

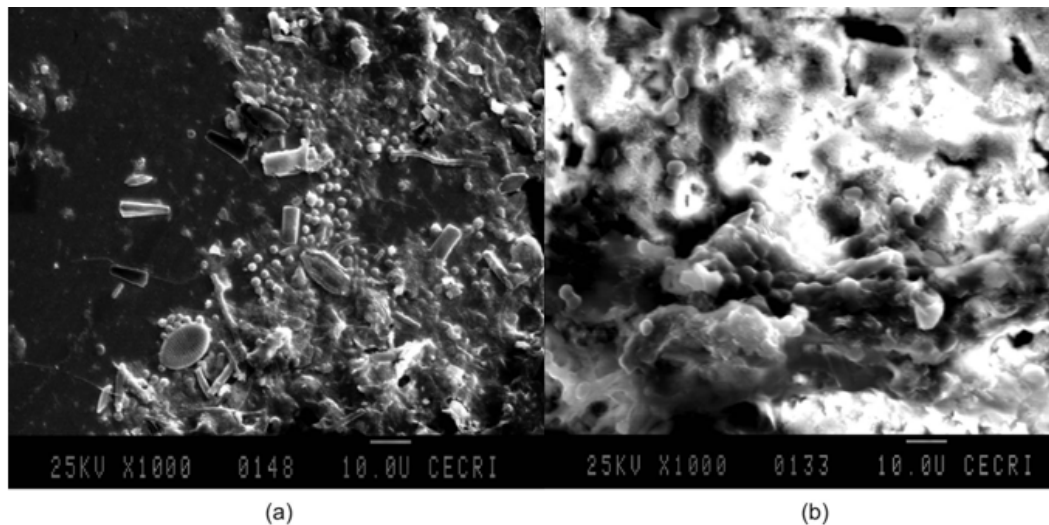


Fig.5. SEM images of uncoupled SS in open-circuit (a) and cathodically polarized to -700 mV (SCE). (b) After 100 h immersion in seawater. Scale bar $\frac{1}{4}$ 10 mm on both images.

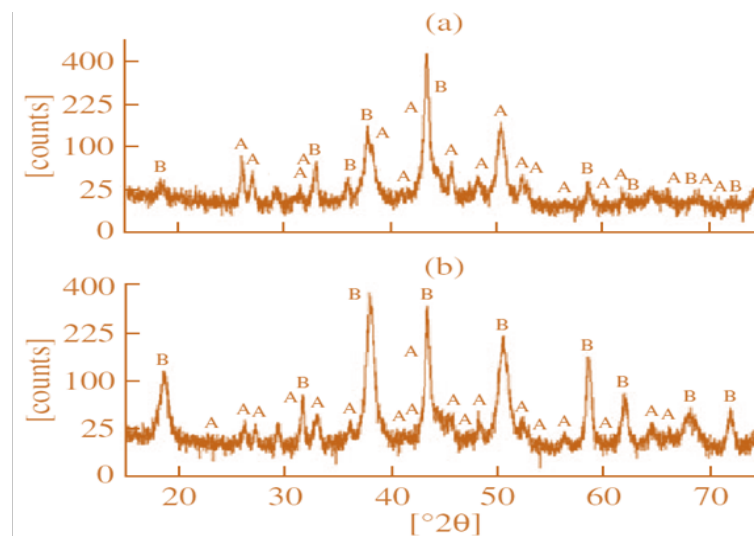


Fig.6. XRD analysis of the deposits formed on 316L stainless steel at potential of (a) -1150 and (b) -1300 mV/SCE. A are the diffraction lines of aragonite, B those of brucite.

The chronoamperometric curves plotted at potential values between -700 and -1300 mV (SCE) indicate the shape and slope of the curve's changes between the potentials of -1050 and -1150 mV (SCE) and the potential of oscillations. The controlling factor for the progression of the reaction is the passage of the dissolved oxygen to and the removal of OH^- ions from the surface. At this potential only a few cathodic current can be ascribed to hydrogen evolution. At -1100 mV/SCE, the natures of the deposits shift from Ca rich phases to brucite that shows the dependence of the current decrease rate to the morphologies and phases type. The SEM images and EDX analysis of deposits formed at different applied cathodic potentials presented in figure 7.

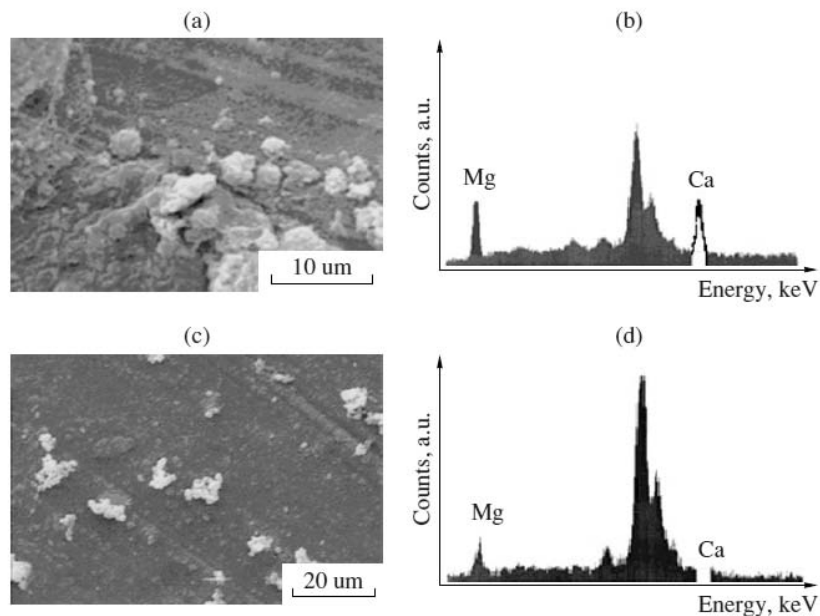


Fig.7. SEM images and EDX analysis of deposits formed on a 316L stainless steel at potential of (a), (b) -1150 and (c), (d) -1300 mV/SCE.

Conclusion:

Among the two tested stainless steels, STS 316 had the most stable electrochemical behavior. In anodic polarization, passivity was remarkably more evident in STS 316 than in STS 304. The pitting and repassivation potentials of 304 and 316 stainless steels were 312, -215 and 330 and -210 mV (SCE) respectively.

Galvanic corrosion rates for LS and Zn coupled to Stainless steel were measured with, and without the accrual of marine biofilms in seawater showed that biofilms caused acceleration of galvanic corrosion rate but calcareous deposits developed rapidly on the SS cathodes and led to the significant reduction of biofilm density.

On 316 Stainless steel substrate, the nature of the deposited phases' shifts from Ca rich phases such as aragonite and calcite to brucite by changing the potential towards cathodic values, but the presence of $Mg(OH)_2$ at the potential less cathodic than water reduction potential (-950 mV/SCE) could be noted. This could be related to high current density values that facilitate the formation of brucite on 316L stainless steel.

References:

- BATES J F. Cathodic protection to prevent crevice corrosion of Stainless Steels in halide media. **Corrosion**, v. 29, n. 1, p. 28-32, 1973.
- DEXTER S C & LaFONTAINE JP. Effect of natural marine biofilms of galvanic corrosion. **Corrosion** v. 54, p. 851–861, 1989.
- DEXTER, S. C. & ZHANG, H. J. Effect of biofilms, sunlight and salinities on corrosion potential and corrosion initiation of stainless alloys. Lewes (DE) University of Delaware. 1991. EPRI Report NP-7275.
- DICKINSON W H, CACCAVO F & LEWANDOWSKI Z. The ennoblement of stainless steel by manganic oxide biofilms. **Corrosion Science**, v. 38, p. 1407–1422, 1996.
- ELIASSEN S. New concept for cathodic protection of offshore pipelines to reduce hydrogen induced stress cracking (HISC) in high strength 13%Cr stainless steels. **Corrosion Engineering, Science and Technology**, v. 39, n.1, p. 31-37, 2004.
- HABIB K. Detection of crevice corrosion by optical interferometry. **Corrosion Science**, v. 42, p. 455-467, 2000.
- HARTT, W. H., CULBERSON, C. H. & SMITH, S. W. Calcareous deposits on metal surfaces in seawater: A critical review. **Corrosion**, v. 40, p. 609–618, 1984.
- HEDAIAT, F., SHAHRABI, T., HOSSEINI, M. G. Sacrificial Cathodic Protection and Crevice Corrosion of Stainless steel in Seawater and Ferric Chloride Solution. In: STAINLESS STEEL WORLD conference. 2005. 8-10 November 2005 Maastricht. Netherlands. p. 1-10
- HEDAIAT, Fr., SHAHRABI, T. & HOSSEINI, M. G. Cathodic Protection and Current Distributions of Crevices Stainless steel in Seawater and Ferric Chloride Solution. In: EUROCORR. 2005. 4 - 8 September 2005. Lisbon. Portugal. P. 1-9.
- JOHNSEN, R. & BARDAL, E. Cathodic properties of different stainless steels in natural seawater, **Corrosion** v.41, p. 296–302, 1985.
- JONES D A. **Principals and Prevention of Corrosion**. 2 ed. Prentice-Hall. 1996. 46p.
- KAIN, R. M. Crevice Corrosion Resistance of Austenitic Stainless Steel in Ambient and Elevated Temperature Seawater. In: Corrosion. 1979. NACE. Paper No. 230.
- KIM, S. J., JANG, S. K. & KIM, J. I. Electrochemical properties and corrosion protection of stainless steel for hot water tank. **The Korean Journal of Chemical Engineering**, v. 21, n. 3, p. 739-745, 2004.
- LEE, T. S. & TUTHILL, A. H. Use of carbon steel to mitigate crevice corrosion of stainless steels in seawater, **Materials Performance**, v. 22, n.1, p. 48-53, 1988.
- LITTLE, B. & WAGNER, P. The interrelationship between marine biofouling and cathodic protection. **Materials Performance**, v. 32, n.2, p. 16-20, 1993
- LITTLE, B., WAGNER, P. & DUQUETTE, D. Microbiologically induced increase in corrosion current density of stainless steel under cathodic protection, **Corrosion**, v. 44, p. 270-274, 1988.
- LUO, J. S., LEE, R. U., CHEN , T. Y., HARTT, W. H. & SMITH, S. W. Formation of calcareous deposits under different modes of cathodic polarization. **Corrosion**, v. 47, p. 189-196, 1991.
- LUO, J. S., LEE, R. U., CHEN, T. Y., HARTT, W. H. & SMITH, S. W. Formation of calcareous deposits under different modes of cathodic polarization. **Corrosion**, v. 47, p. 189-196, 1991.
- LYE, R. E. Current Drain to Cathodically Protected Stainless Steels in Seawater. In: Corrosion. 1988. NACE. Houston, TX. Paper No. 39
- MALIK, A. U. & Al FOZAN, SALEH. Localized corrosion of AISI 316L SS in Arabian Gulf seawater. **Desalination**, v. 97, p. 199-212, 1994.

- MELE, M. F. L. de. & GOMEZ DE SARAVIA, S. G. Interrelationships between bacterial biofouling, calcareous deposits and stainless steel under cathodic protection. **Corrosion Review**, v. 12, p. 111-128, 1994.
- MOLLER, G. E. The Successful Use of Austenitic Stainless Steels in Seawater. In: 8th Offshore Technology Conference. 1976. Paper No. OTC 2699.
- OLDFIELD, JOHN W. Test techniques for pitting and crevice corrosion resistance of stainless steels and nickel base alloys in chloride containing environments. **International Materials Reviews**, v. 32, n. 3, p. 1-18, 1987.
- SARLAK, M., SHAHRABI, T., & ZAMANZADE, M. Investigation of Calcareous Deposits Formation on Copper and 316L Stainless Steel under Cathodic Polarization in Artificial Seawater. **Protection of Metals and Physical Chemistry of Surfaces**, v. 45, n. 2, p. 216–222, 2009.
- SCOTTO, V., DI CINTIO, R. & MARCENARO, G. The influence of marine aerobic microbial film on stainless steels corrosion behavior. **Corrosion Science**, v. 25, p. 185-194, 1985.
- SEDRIKS J. **Corrosion of Stainless Steels**. 1 ed. Wiley Interscience publication. 1996. 14p.
- SHAHRABI, T., HEDAIAT, Fr. & HOSSEINI, M. G. Sacrificial Cathodic Protection against Crevice Corrosion of Austenitic Stainless Steels in Seawater. In: EUROCORR. 2005. 4 - 8 September. Lisbon. Portugal. p. 1-8
- SINHA, A. K., BHAKTA, U. C. & et al. Prevention of crevice corrosion of SS304 in condensers of power plants by sacrificial cathodic protection. In: proc. Int. conf. on corrosion CONCORN.1997. December 3-6. Mumbai. India. p. 1103-1120
- WIENG, S. M., OSVOLL H. & GARTLAND, P. O. Efficient cathodic protection to stainless steel small bore tubing. In: Corrosion. 2007. NACE. Houston, TX. Paper No. 07078.

Corresponding author: F. Hedaiat (fa_hedaiat@yahoo.com)